Push-Pull Resoswitch Communication Receiver

Qiutong Jin, Kevin Zheng, and Clark T.-C. Nguyen
Berkeley Sensor & Actuator Center
Dept. of Electrical Engineering and Computer Sciences
University of California, Berkeley, California, USA
qiutong-jin@berkeley.edu

***Summary*—A squegging-free all-mechanical communication receiver capable of receiving and demodulating up to 1 kbit/s full FSK inputs at -67.4 dBm sensitivity is demonstrated using push-pull operation of two frequency-spaced micromechanical resoswitches. Here, the use of pull-up and pull-down resoswitches is key to permitting well-controlled charging and discharging of a load capacitor and obviating the bleed resistor used in previous resoswitch receivers, reducing greatly the power draw when processing valid bits. The use of two resoswitches in concert not only permits reception of both mark and set FSK inputs to reap the benefits of full FSK reception not achieved by previous demonstrations, but also by removing squegging removes transition glitches that plagued the stability, i.e., degraded the Allan deviation, of previous resoswitch-based clock receivers.**

Keywords—MEMS switch, resonator, FSK, OOK, low power, zero power, squegging, bit rate, gold metal.

I. Introduction

All-mechanical communication/clock receivers employing micromechanical resonant switches, a.k.a., resoswitches [1], *cf.* Fig. 1, to receive On-Off Keyed (OOK) or Frequency Shift Keyed (FSK) modulated input signals and demodulate them (but before this work only in OOK fashion) have the unique ability to listen in standby for incoming communication inputs without consuming power [2][3]. Such resoswitches differ from conventional static switches in that instead of closing once to transfer charge, they dynamically impact two conductors, which provides both reliability and frequency addressability advantages. Recent use of stored resonance energy to demonstrate bit rates up to 8 kbit/s [4] now allows such receivers to move beyond low bit rate applications, e.g., cross-continent label updates, to higher bit rate ones, possibly voice communications or firmware updates.

Unfortunately, squegging, whereby non-ideal impacts induce phase shifts that debilitate the resonance drive efficiency, causes missed impacts and output frequency instability [5]. Pursuant to eliminating squegging and enabling full FSK demodulation (with its bit error rate benefits), this work employs two frequency-spaced resoswitches in a push-pull configuration (*cf.* Fig. 2) to eliminate squegging and thereby achieve glitch-less 100-1000 bit/s output waveforms with near brick wall steps that offer substantially better stability than previous resoswitch receivers.

II. Resoswitch Design

The resoswitches shown in Fig. 1 essentially comprise Very Low Frequency (VLF, 3-30 kHz), folded-beam comb-driven resonators [5] for which their shuttles have been modified with pointed impactors that impact nearby soft electrodes [6] upon

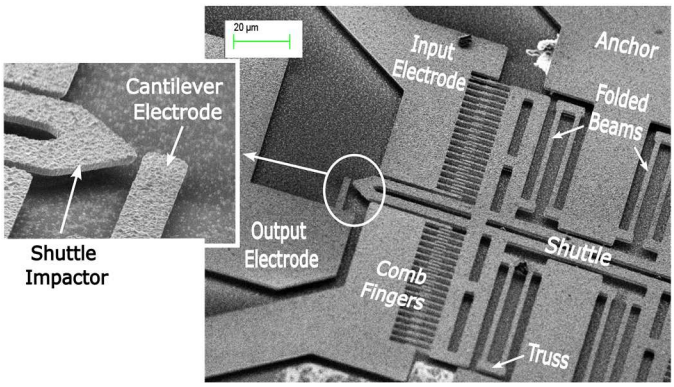

Fig. 1. SEM of a gold resoswitch identifying important features. Upon application of a dc-biased sinusoid at the device resonance frequency to the input comb-finger electrode, the movable suspended shuttle vibrates to impact the output electrode, periodically closing the shuttle-to-output switch.

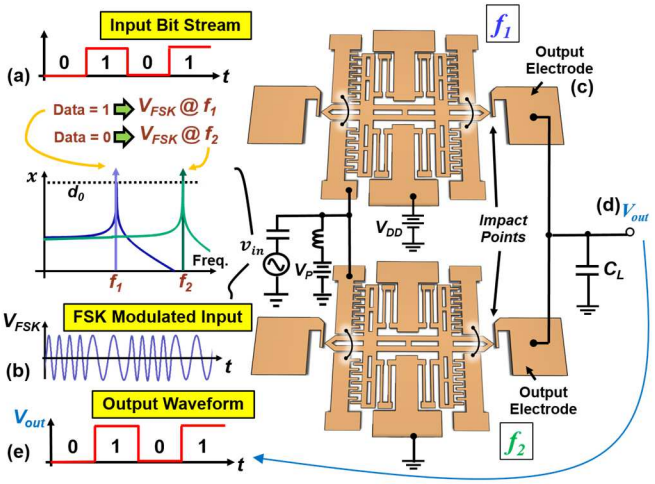

Fig. 2. Illustrative summary of a push-pull all-mechanical zero quiescent power FSK receiver. Here, the (a) input bit stream is (b) FSK-modulated into an off-resonance signal to represent a '0' or an on-resonance signal to denote a '1'. Reception of a '1' at the input electrode induces resonance vibration of the top structure, in turn instigating impacting of the shuttle to the output electrode at (c). Impacting then periodically transfers charge from V_{DD} to the output load capacitor (d) C_L, eventually charging it to V_{DD}, which corresponds to a '1'. Any '0' input received afterwards stops resonant impacting of the top resonator and instigates it in the bottom one, which impacts to connect the output node to ground, allowing C_L to discharge to ground, denoting a '0'. In this way, the input bit stream is faithfully reproduced at the output, as shown in (e).

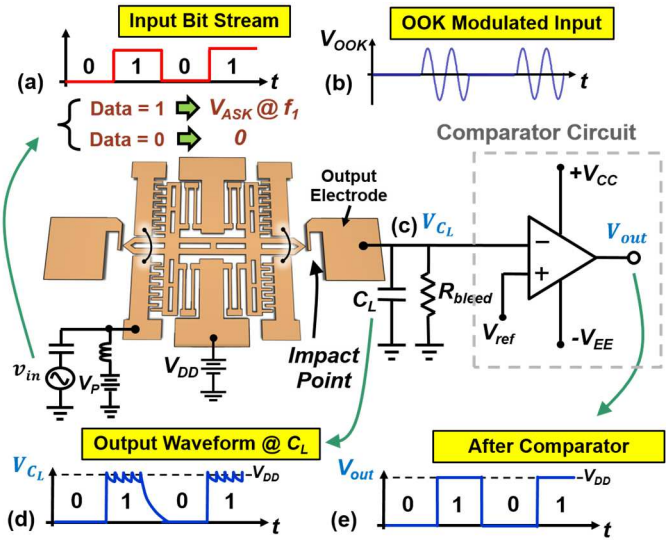

Fig. 4. Illustrative summary of a low-frequency all-mechanical zero quiescent power OOK receiver. Here, the (a) input bit stream comprises a (b) OOK-modulated on-resonance carrier signal that drives the device into resonance vibration, instigating shuttle-to-electrode impacts during "on" periods that then charge (c) C_L to deliver a (d) output high. During "off"' periods, the resoswitch does not move, so does not impact the output, allowing bleed resistor R_{bleed} to discharge C_L to 0V (i.e., output low). Constant current bleed by R_{bleed} becomes problematic from both stability and processing power consumption perspectives.

excitation to sufficient shuttle displacement, achieved via resonance vibration. The device design is such that shuttle impactor-to-electrode impacting occurs only during resonance vibration, at which point current flows through the periodic conductive path between the shuttle and electrode. In previous renditions of resoswitch receivers, such as shown in Fig. 3 [6], charge flows through the periodic conductive path between the power supply V_{DD} and the electrode to charge the waiting load capacitor C_L (and the output) to voltage V_{DD}. On the other hand, non-resonance inputs do not induce sufficient displacement for impacts, so no charge flows into C_L. If C_L held any charge, the bleed resistor R_{bleed} in Fig. 3 would drain it, sending the output voltage to ground.

TABLE I summarizes the dimensions and materials used to achieve the indicated performance via the devices of this work. The gold structural material (that limits the Q to ~500), 500-nm impactor-to-electrode gap, and 1-µm comb-finger gaps per side, all contribute to a receiver sensitivity of -67.4 dBm.

III. The Problem With Squegging

Ideally, a continuous resonance sinusoidal input voltage would yield displacement and output waveforms as shown in Fig. 4(a)-(c), where each top cycle of the displacement waveform impacts the electrode and thereby maintains charge on C_L to overcome continuous discharging by R_{bleed} (in the Fig. 3 circuit), leading to the depicted sawtooth-like waveform.

Unfortunately, however, actual impacts are not so ideal. Rather, as shown in Fig. 4(d), each impact can de-phase the shuttle motion so that the displacement sinusoid is no longer 90° phase-shifted from the input force sinusoid, reducing the drive efficiency. The shuttle vibration amplitude then drops in response,

TABLE I Resoswitch Dimensions And Material Properties

	Row No.	Parameter	Value	Unit
Dimensional Variables		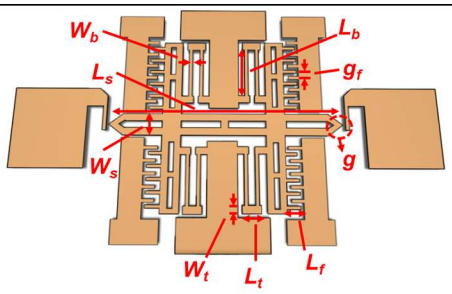		
Designed/Fabricated/Given	1	Resonator Shuttle, L_s	160	µm
	2	Resonator Shuttle Width, W_s	15	µm
	3	Resonator Truss Length, L_t	10	µm
	4	Resonator Truss Width, W_t	5	µm
	5	Resonator Beam Length, L_b	60	µm
	6	Resonator Beam Width, W_b	1.5	µm
	7	Resonator Finger Length, L_f	10	µm
	8	Resonator Finger Width, W_f	1	µm
	9	Resonator Finger Spacing, g_f	1	µm
	10	Impactor-to-Electrode Gap, g	500	nm
	11	Gold Film Thickness, h	1.07	µm
	12	Finger Number Per Side, N	38	---
	13	Young's Modulus, E	79	GPa
	14	Density, ρ	19300	kg/m^3
Measured/ Calculated	15	Measured Frequency, f_0	22.8	kHz
	16	Measured Quality Factor, Q	502	---
	17	V_P Used in Measurement	12	V
	18	Resonator Shuttle Mass, m_s	3.73×10^{-11}	kg
	19	Resonator Truss Mass, m_t	4.13×10^{-12}	kg
	20	Resonator Beam Mass, m_b	1.49×10^{-11}	kg
	21	Resonator Mass, m_r	1.28×10^{-10}	kg
	22	Resonator Stiffness, k_r	2.64	N/m
	23	Resonance Frequency, f_0	22.8	kHz
	24	Motional Resistance, R_x	314	MΩ
	25	Sensitivity, S	-67.4	dBm

leading to missed impacts. The force and displacement eventually restore their 90° phase shift, re-establishing an efficient resonance drive force that drives the shuttle back to impacting, upon which the cycle of impacting, missing for a few cycles, impacting, missing for a few cycles, etc., continues. This behavior, depicted in the measured waveform of Fig. 4(e), is squegging.

If impacts interrupt for only a few cycles, then squegging is largely benign. Squegging becomes consequential when the de-phasing is such that missed cycles go on long enough for the bleed resistor R_{bleed} to pull down the output voltage into the range considered an input low, which would then inadvertently switch the next stage, e.g., to a high if the next stage were an inverter, causing an error in a data application, or destabilizing the frequency in a frequency control application.

Given the degree to which squegging can compromise applications, numerous solutions to squegging have been proposed, with varying degrees of success, but none of them per-

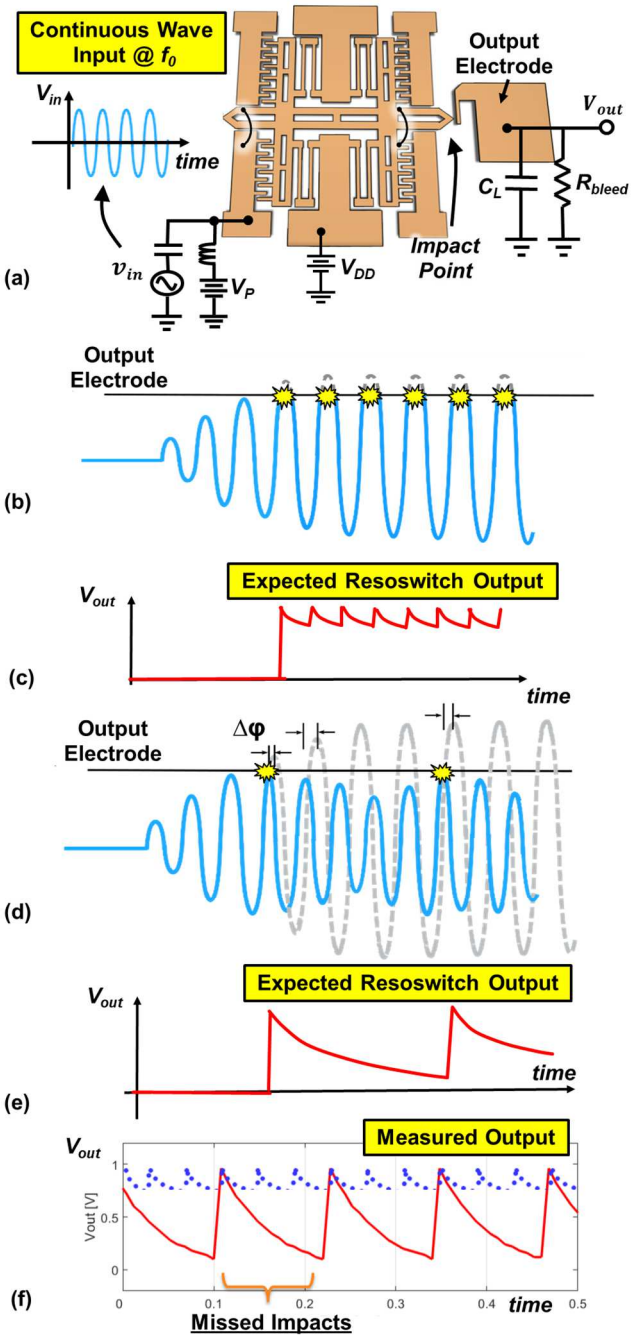

Fig. 4. Illustrations depicting one mechanism behind squegging. Here, a continuous wave input at resonance frequency f_0 drives the resoswitch device (a). Ideally, the resoswitch shuttle would impact the output electrode periodically (b) and maintain the 90° phase-shift between displacement and input force needed for efficient drive, generating the output waveform in (c). Unfortunately, impacts introduce phase shifts that pull the displacement and force away from 90° (d), reducing the drive efficiency and causing missed impacts until the phase recovers to restore drive efficiency and induce impacting once again. Less frequent impacts lead to an output waveform with much deeper sawtooths, as depicted in (e) and the measured waveform of (f).

fect. These include contact engineering, e.g., hard vs soft contacts, ensuring device symmetry, impact gap design, and input thresholds [6][7][8]. These solutions generally require significant design modifications that often must be traded off with other performance variables.

A much better solution arises from the recognition that squegging-induced errors derive mainly from the presence of the bleed resistor R_{bleed}. Specifically, in Fig. 3, because the bleed resistor continuously sinks current to ground, the shuttle must continuously impact the electrode to restore the charge across C_L and maintain a high output voltage. This would not be necessary if C_L could be discharged (and charged) not continuously, but only when needed, as happens in push-pull circuit topologies.

IV. Push-Pull Receiver Topology and Operation

Fig. 2 and Fig. 3 compare the new push-pull FSK receiver topology with the previous single-resoswitch OOK one of [4]. One obvious difference is the use of two resoswitches in the former, one with switch shuttle tied to the supply voltage V_{DD}, the other tied to ground. Here, when the upper "pull-up" resoswitch activates, it creates a (periodic) conductive path from V_{DD} to the output load capacitor C_L and charges it very similarly to the PMOS device in a static CMOS inverter. When the bottom "pull-down" resoswitch impacts, it then shunts the charge on C_L to ground, sending the output voltage to ground.

Like a static CMOS inverter, the circuit operates most efficiently if the pull-up and pull-down devices are never on at the same time—something not easily achievable in CMOS, but very achievable using resoswitches. Indeed, unlike CMOS, the resoswtiches in Fig. 2 can be activated by frequency inputs, where different resonance frequencies of the pull-up and pull-down devices offer a buffer zone between on and off frequencies, ideally guaranteeing the devices operate distinctly. Here, unlike the bleed resistor-loaded case of Fig. 3, the push-pull circuit of Fig. 2 eliminates competition between pull-up and pull-down, so can minimize the amount of charge needed to set an output high or low on C_L, thereby saving processing power. Removal of competition in the push-pull topology also permits brick wall transitions brought on by unimpeded charging or discharging of C_L, all without any need for the comparator in the Fig. 3 circuit.

Perhaps most importantly, since there is no bleed resistor constantly pulling the voltage down, any squegging events (i.e., missed impacts) have no consequence. The circuit is ideally immune to squegging, unlike the circuit of Fig. 3, where the measured output in shows how a squegging event can introduce an extra output transition, which then shifts the frequency, causing instability.

V. Measured Results

Fig. 1 presents the SEM of an all-gold resoswitch used in this work, fabricated using the process summarized in Fig. 6 that replaces the oxide mold of [2] with a simpler photoresist mold. Two such devices were inserted into a 10 mTorr Lakeshore FWPX Vacuum Probe Station and hooked into a circuit like that of Fig. 2, with ports to an outside function generator and oscilloscope that apply inputs and measure performance, respectively. For comparison, the single-device circuit of Fig. 3 was also constructed and measured.

Fig. 5 and Fig. 7 plot measured data for the Fig. 3 and Fig. 2 circuits, respectively. Here, the resoswitch activating input

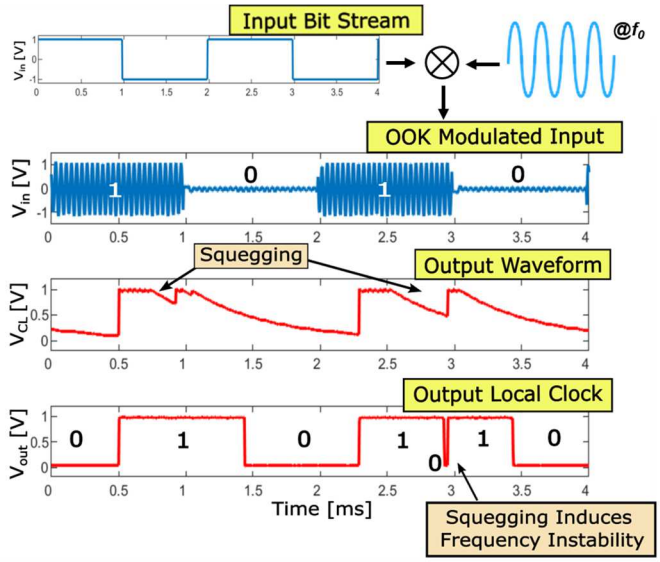

Fig. 5. Measured OOK input, C_L output, and comparator output waveforms for the single-device circuit of Fig. 3 followed by a comparator (amplifier), as in [5]. (V_{CL} is the voltage across C_L, while V_{CLK} is the output of the comparator.) Here, squegging induces a deep drop in V_{CL} around 3 ms that then causes the comparator output V_{CLK} to switch in error.

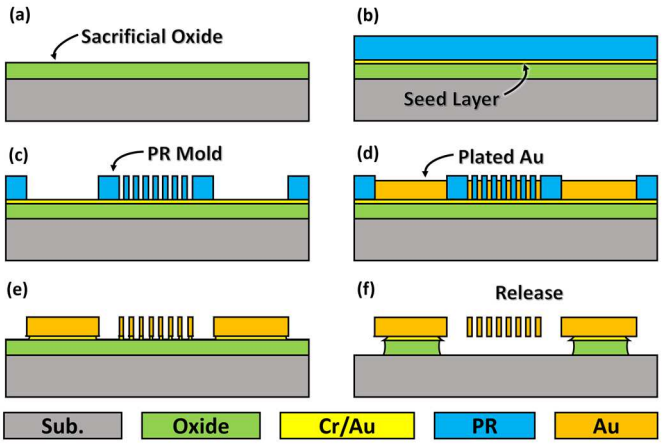

Fig. 6. One-mask gold resoswitch fabrication process that starts with (a) deposition of sacrificial oxide onto a blank silicon wafer using LPCVD, then (b) sputter deposition of Cr/Au to promote adhesion between oxide and gold and serve as an electroplating seed layer. A thick layer of photoresist is then deposited and patterned to form a mold with cross-section as in (c), after which gold electroplating through the mold in a cyanide-based solution forms the structure in (d). Removal of the photoresist mold to yield (e) and a release in vapor-phase HF yields the final suspended movable structure cross-section in (f).

frequencies are 22.85 kHz and 25.21 kHz for the pull-up and pull-down devices, respectively, which also correspond to the mark and space frequencies of the FSK input. Immediately discernible are the sharp, brick-wall output transitions across C_L (before any comparator, in this case flip-flop, amplification) of the push-pull circuit relative to the Fig. 3 single-device circuit before the comparator. The former's C_L voltage V_{CL} waveform is also much smoother than the singe-device one, which suffers from continuous current bleed that causes jagged tops, as well as a squegging-induced deep dive leading to an unwanted transition at the flip-flop output that contributes to frequency instability. Meanwhile, if any squegging occurs in the push-pull circuit of Fig. 2, it is not evident in Fig. 7, which attests to the push-pull circuit's immunity against squegging.

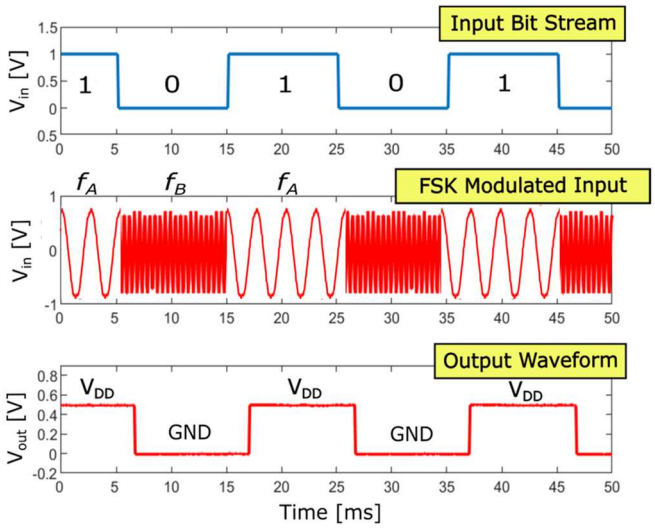

Fig. 7. Measured FSK input and practically perfect output (despite possible squegging) of the push-pull resoswitch receiver of Fig. 2. No comparator is needed here to achieve the "brick wall" output waveform.

VI. Conclusions

By eliminating the impact of squegging, the demonstrated push-pull circuit solves perhaps the most limiting aspect of all-mechanical resoswitch receivers—reliability and bit error rate—and further improves their communication efficiency and robustness by permitting full FSK operation. This result, together with recent bit rate increases, now brings all-mechanical resoswitch receivers much closer to practical commercial applications that can withstand transistor-unfriendly environments while largely eliminating battery drain concerns.

References

[1] Y. Lin, W. -C. Li, Z. Ren, and C. T.-C. Nguyen, "The micromechanical resonant switch ("Resoswitch")," in *Hilton Head*, 2008, pp. 40-43.

[2] R. Liu, J. Naghsh Nilchi, T. Naing and C. T.-C. Nguyen, "Zero Quiescent Power VLF Mechanical Communication Receiver," in *Transducers*, Anchorage, 2015, pp. 129–132.

[3] C. -P. Tsai, Y. -Y. Liao and W. -C. Li, "A 125-kHz CMOS-MEMS Resoswitch Embedded Zero Quiescent Power OOK/FSK Receiver," in *Proc. 33rd IEEE International Conference on Micro Electro Mechanical Systems (MEMS)*, 2020, pp. 106-109.

[4] Q. Jin, K. Zheng and C. T.-C. Nguyen, "Bit rate-adapting resoswitch," in *Proc. 2022 International Electron Devices Meeting (IEDM)*, 2022, pp. 16.5.1-16.5.4.

[5] R. Liu, J. N. Nilchi and C. T.-C. Nguyen, "RF-powered micromechanical clock generator," in *2016 IEEE Int. Freq. Control Symp.*, 2016, pp. 1-6.

[6] R. Liu, J. N. Nilchi and C. T. -C. Nguyen, "CW-powered squegging micromechanical clock generator," in *Proc. 30th IEEE International Conference on Micro Electro Mechanical Systems (MEMS)*, 2017, pp. 905-908.

[7] R. L. Jackson, I. Green, and D. B. Marghitu, "Predicting the coefficient of restitution of impacting elastic-perfectly plastic spheres," *Nonlinear Dynamics*, 60(3), pp. 217-229, 2010.

[8] Y. Lin, R. Liu, W. -C. Li and C. T. -C. Nguyen, "Polycide contact interface to suppress squegging in micromechanical resoswitches," in *Proc. 27th IEEE International Conference on Micro Electro Mechanical Systems (MEMS)*, 2014, pp. 1273-1276.